Effect of Sonication on the Disruption of Gram-Negative Bacterial Biofilms Associated with Prosthetic Joint Infections (PJI) at Different Maturation Stages: An *In Vitro* Study

Natally Dos Santos Silva *, Cynthia Regina Pedrosa Soares, Fábio André Brayner dos Santos, Paulo Sérgio Ramos de Araújo

Posted Date: 12 December 2025

doi: 10.20944/preprints202512.1160.v1

Keywords: biofilm; sonication; gram-negative bacteria; prosthetic joint infection; *Escherichia coli*; Pseudomonas aeruginosa

 doi:10.20944/preprints202512.1160.v1

Article

Effect of Sonication on the Disruption of Gram-Negative Bacterial Biofilms Associated with Prosthetic Joint Infections (PJI) at Different Maturation Stages: An *In Vitro* Study

Natally Dos Santos Silva [1,*], Cynthia Regina Pedrosa Soares [2], Fábio André Brayner dos Santos [2] and Paulo Sérgio Ramos de Araújo [2]

[1] Department of Tropical Medicine – Federal University of Pernambuco - UFPE, Block A, Ground Floor, Hospital das Clínicas, Av. Prof. Moraes Rego, 1235, University City, Zip Code 50670-901, Recife, Brazil
[2] Department of Parasitology - Aggeu Magalhães Institute - IAM - Fiocruz-PE, Avenida Professor Moraes Rego, s/n, Cidade Universitária, CEP 50.740-465, Recife, Brazil
* Correspondence: natallydossantos8@gmai.com; Tel.: +55 81998082148.

Abstract

Background/Objectives: Periprosthetic joint infections (PJIs) remain one of the most challenging complications after arthroplasties due to the ability of pathogens to form biofilms on implant surfaces. Although staphylococci predominate, Gram-negative bacilli, have increasingly been associated with more aggressive clinical courses and diagnostic failure. This study aimed to evaluate the structural characteristics and maturation of *E. coli* and *P. aeruginosa* biofilms and to assess the effectiveness of a standardized sonication protocol in disrupting these biofilms and releasing viable cells. **Methods:** Biofilms of *E. coli* (ATCC 25922) and *P. aeruginosa* (ATCC 53278) were grown on polyethylene catheter segments for 24, 48, and 72 hours. Morphological and structural features were assessed by scanning electron microscopy. A standardized sonication protocol was then applied to evaluate its ability to disrupt the extracellular polymeric matrix. Viability of released cells was confirmed by culturing aliquots of the sonication fluid on BHI agar. Biofilms were produced in triplicate for each time point. **Results:** Both species formed increasingly dense and structured biofilms over time. Mature biofilms exhibited markedly thicker EPS layers compared to 24-h biofilms. *P. aeruginosa* developed highly complex, multilayered matrices, while *E. coli* produced characteristic but less elaborate biofilm structures. Sonication consistently disrupted immature and mature biofilms of both organisms, fragmenting the matrix and releasing individual or small clusters of bacterial cells. Cultures from the sonication fluid demonstrated that bacterial cells remained viable following the procedure. **Conclusions:** The standardized sonication protocol effectively disrupted Gram-negative biofilms at different maturation stages and released viable microorganisms, reinforcing its value as a complementary diagnostic tool for PJIs, especially in chronic or low-grade infections where conventional culture methods show reduced sensitivity.

Keywords: biofilm; sonication; gram-negative bacteria; prosthetic joint infection; *Escherichia coli; Pseudomonas aeruginosa*

1. Introduction

Periprosthetic joint infections represent the most severe complication of arthroplasties, with substantial impact on patient morbidity, mortality, and healthcare costs [1,2]. Although *Staphylococcus aureus* and coagulase-negative staphylococci remain predominant etiological agents, Gram-Negative Bacillis (GNBs), particularly *Escherichia coli* and *Pseudomonas aeruginosa*, have increasingly been recognized as relevant causes of PJIs, often associated with more aggressive clinical courses and reduced therapeutic responsiveness [3]. In all these scenarios, the ability of these

 doi:10.20944/preprints202512.1160.v1

organisms to form biofilms on implant surfaces is a critical determinant of infection persistence, conferring protection against host immune mechanisms and significantly reducing antimicrobial efficacy.

Biofilm maturation follows a structured progression consisting of: (1) reversible adhesion, (2) irreversible adhesion, (3) cellular proliferation with microcolony formation, (4) maturation with production of a complex extracellular matrix, and (5) dispersion [4–6]. As biofilms mature, bacterial tolerance to antimicrobials increases, and microbial detection by conventional methods becomes progressively more difficult. Consequently, diagnostic failures and false-negative results are common, particularly in chronic infections evaluated solely by Periprosthetic Tissue Culture (PTC), still regarded as the diagnostic gold standard [5–7].

To overcome these limitations, physical methods for biofilm disruption have been incorporated as pre-analytical steps. Among them, sonication—first proposed by Trampuz *et al*. (2007), showed improved accuracy compared with PTC across different experimental and clinical settings [8,9]. Since then, multiple sonication protocols, varying in duration, frequency, temperature, and sample processing, have been proposed and compared with the gold standard [8,10,11]. However, methodological heterogeneity across studies has resulted in inconsistent evidence regarding the actual diagnostic gain provided by sonicated fluid culture.

Although several studies have investigated sonication as a diagnostic tool, most focus on Gram-positive pathogens, and few provide direct Scanning Electron Microscopy (SEM) visualization of the structural effect of sonication on Gram-negative biofilms at different maturation stages [8,10,11].

In a previous publication [11], we addressed this issue and proposed a theoretical framework for the standardization of a sonication protocol aimed at achieving high sensitivity and specificity in the microbiological diagnosis of implant-associated infections, including PJIs. However, the practical application of this protocol had not yet been evaluated. Therefore, the aim of the present study was to conduct an in vitro investigation of the effect of sonication on the disruption of biofilms formed by Gram-negative bacilli associated with PJIs, across different stages of biofilm maturation, using SEM.

2. Results

2.1. Temporal Development and Maturation of Bacterial Biofilms

All strains tested in this study, *Escherichia coli* (ATCC 25922) and *Pseudomonas aeruginosa* (ATCC 53278), successfully formed biofilms following the proposed methodology, exhibiting the characteristic structural organization: dense, highly hydrated aggregates separated by interstitial spaces or water channels, forming a three-dimensional (3D) architecture of extracellular polymeric substance (EPS). This matrix is composed of polysaccharides, proteins, lipids, DNA, and RNA [12], but appears as an amorphous material under SEM. Across all incubation periods evaluated (24, 48 and 72 hours), each strain demonstrated distinct stages of biofilm maturation, with progressive increases in density, complexity, and 3D organization over time (Figure 1).

Among the Gram-negative bacteria, *E. coli* exhibited, at 24 h, a structure with well-individualized and dispersed cells surrounded by a thin amorphous layer, consistent with the adhesion phase and the onset of microcolony formation. At 48 h and 72 h, the biofilms displayed more aggregated bacteria embedded within an increasingly dense amorphous matrix. By 72 h, many cells were partially submerged within this structure, a hallmark of a mature biofilm (Figure 1A–C).

The 24-h biofilm of *P. aeruginosa* similarly showed early adhesion of irregularly arranged rod-shaped cells and the initial accumulation of visible matrix. At 48 h, the

 doi:10.20944/preprints202512.1160.v1

biofilm exhibited larger and denser clusters, displaying heterogeneous organization with small 3D elevations separated by uncovered areas. By 72 h, a mature biofilm was evident, characterized by a compact cellular mass covered by a thick, continuous EPS matrix that extended across nearly the entire surface (Figure 1D–F).

In general, *P. aeruginosa* biofilms were consistently thicker and more structured at all time points analyzed, compared to those of *E. coli*.

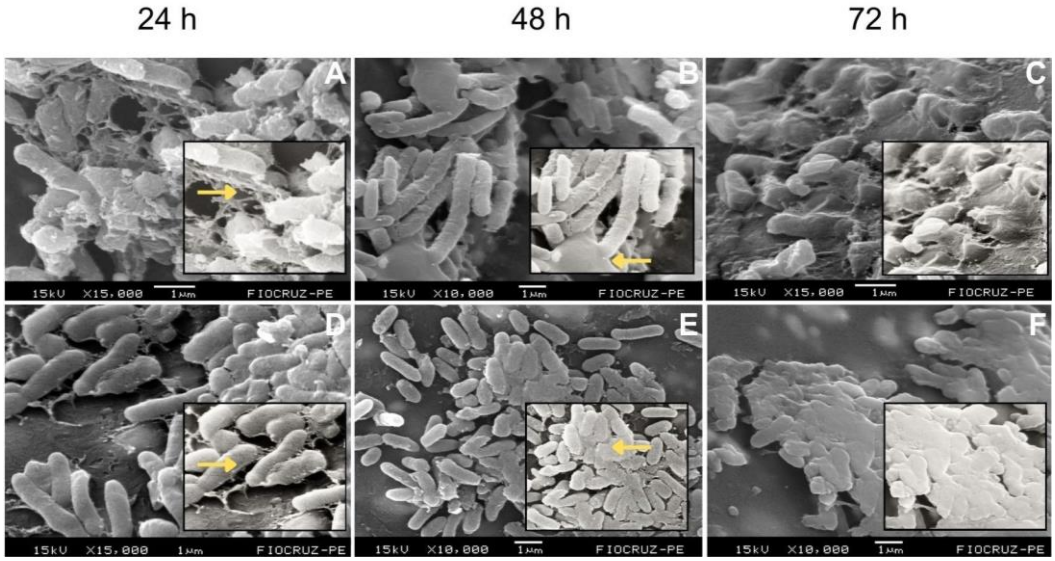

Figure 1. Temporal evolution of biofilm formation by *Escherichia coli* (A–C) and *Pseudomonas aeruginosa* (D–F) at 24, 48 and 72 hours. The micrographs show the transition from isolated cells to microcolonies, followed by the development of an amorphous extracellular matrix (EPS) and a mature three-dimensional architecture. Scale bars are shown within each panel.

2.2. Effect of Sonication on Biofilm Disruption

Regarding the effect of the sonication protocol on the biofilm structure of the strains studied, we observed that, in all of them, sonication was able to disrupt the extracellular matrix, promoting disaggregation and releasing bacterial cells from the biofilm structure. In the *E. coli* biofilms, sonication effectively disrupted the biofilm at all three maturation stages, eliminating the structural organization observed in the controls (Figure 2). In the 24-hour biofilm, sonication already resulted in a clear loss of the initial organization, with more dispersed cells and the absence of compact aggregates. In the 48-hour biofilm, this effect persisted, causing fragmentation of the developing structure and reducing the presence of adherent cellular layers. In the mature 72-hour biofilm, a greater degree of structural destruction was visible, consistent with the higher complexity of the 3D architecture in the control, with extensive extracellular matrix damage, disrupted areas, residual filamentous structures, and dispersed rods or rods still attached to fragments of the ruptured matrix (Figure 2F).

For *P. aeruginosa* biofilms, the effect of the sonication protocol was also evident at all maturation stages (Figure 3). In well-structured biofilms, such as those at 48 hours, sonication led to complete fragmentation, with predominance of individual cells and absence of a visible matrix (Figure 3E). A similar pattern was observed in the 72-hour biofilm: while controls displayed a dense and mature architecture, the sonicated biofilms showed dispersed cellular aggregates and only small remnants of matrix (Figure 3F).

 doi:10.20944/preprints202512.1160.v1

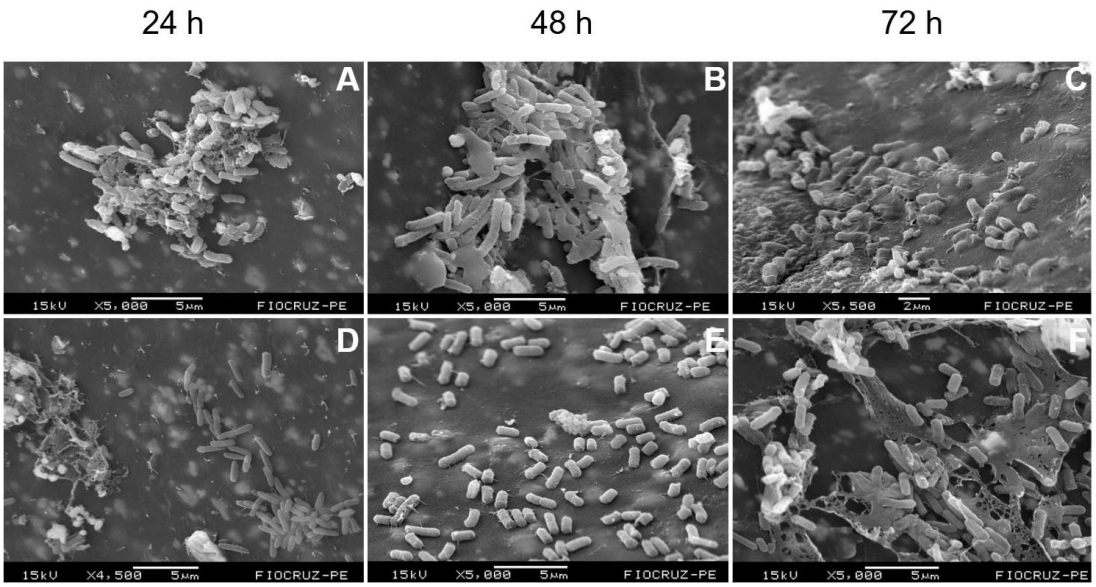

Figure 2. Structural effect of the sonication protocol on *Escherichia coli* biofilms at 24, 48 and 72 hours. Panels A–C show non-sonicated biofilms at 24, 48 and 72 h, respectively, while panels D–F depict the corresponding sonicated samples, illustrating matrix disruption, reduced aggregation, and increased dispersion of bacterial cells. Scale bars are shown within each panel.

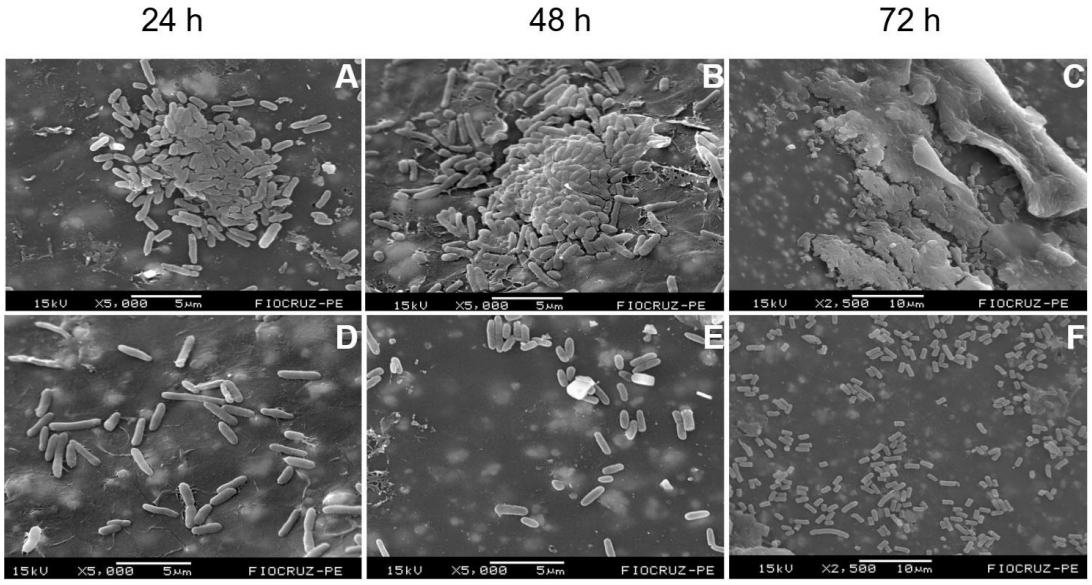

Figure 3. Structural effect of the sonication protocol on *Pseudomonas aeruginosa* biofilms at 24, 48 and 72 hours. Panels A–C show non-sonicated biofilms at 24, 48 and 72 h, respectively, while panels D–F depict the corresponding sonicated samples, illustrating matrix disruption, reduced aggregation, and increased dispersion of bacterial cells. Scale bars are shown within each panel.

As demonstrated in the results described above, sonication promoted the release of microbial cells from the biofilm into the sonication fluid, further evidenced by the formation of a visible pellet after centrifugation of the catheter segments together with the rinsing fluid used in the protocol (Figure 4A). The fluid from all samples was subsequently cultured on Brain Heart Infusion (BHI) agar plates, and after 18–24 hours of incubation at 37 °C, well-defined bacterial colonies were observed (Figure 4B), confirming that the released cells remained viable for growth following the procedure.

 doi:10.20944/preprints202512.1160.v1

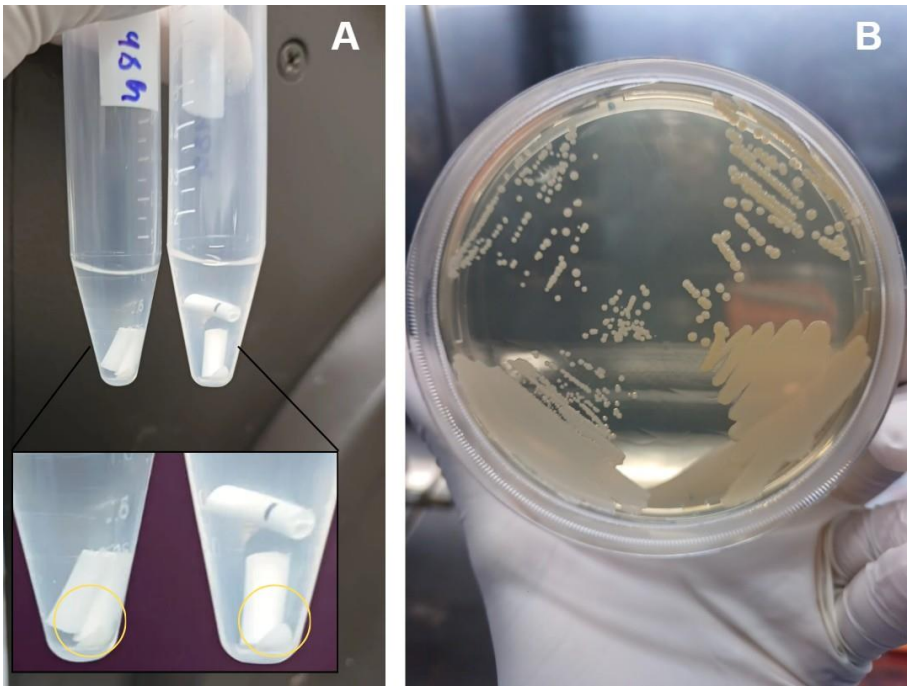

Figure 4. Recovery of viable bacteria after sonication. (A) Pellet formed after centrifugation of the sonication fluid collected from the catheter segments, indicating the release of microbial material. (B) Growth of bacterial colonies on BHI agar after 18–24 h of incubation at 37 °C, demonstrating the viability of the cells detached by sonication.

3. Discussion

Biofilms are complex three-dimensional structures formed when microorganisms irreversibly adhere to a surface and produce an extracellular polymeric matrix [13]. Biofilm formation plays a central role in the pathogenesis of implant-associated infections, particularly PJIs, where the biofilm both enables microbial evasion of host immune responses and limits the effectiveness of antimicrobial therapy, in addition to reducing the sensitivity of conventional culture-based diagnostic methods [13,14]. It is important to note that biofilm complexity is closely linked to the chemical composition of its matrix, which varies among bacterial species. While most studies have focused on biofilms formed by Gram-positive pathogens, there remains a significant gap in our understanding of biofilm characteristics in Gram-negative bacteria within the context of PJIs [12,15].

In this study, we observed that the laboratory strains of Gram-negative bacilli (GNB) readily formed biofilms, behaving as efficient biofilm producers. *Pseudomonas aeruginosa* developed robust biofilm structures (Figure S11), consistent with previous reports showing its superior growth and biofilm-forming capacity both *in vitro* and *in vivo* [15,16]. It is well established that *P. aeruginosa* forms exceptionally complex and resilient biofilms due to a combination of structural and regulatory features, including an extracellular matrix composed of three major exopolysaccharides—alginate, Psl, and Pel—which act synergistically to generate a dense, cohesive, and highly stable architecture. In addition, gene regulation via cyclic di-GMP and quorum sensing coordinates the expression of genes necessary for increased density, maturity, and three-dimensional structuring [12].

E. coli, in turn, efficiently formed biofilms with a characteristic architecture (Figure S5). However, these structures were less organized and exhibited lower architectural complexity compared with the biofilms produced by *P. aeruginosa* [4,12].

Although this study employed central venous catheter segments made of polyethylene (a material also used as an articulating surface in combination with metallic or ceramic components in orthopedic prostheses) *P. aeruginosa*, as well as *Staphylococcus aureus*, has already been shown to form biofilms on a wide range of prosthetic materials (e.g., cobalt–chromium, oxinium, and ceramic femoral heads). This indicates that biofilm formation is not restricted to a single type of prosthetic

 doi:10.20944/preprints202512.1160.v1

surface and is highly relevant in the real clinical setting [17]. Moreover, while GNB are increasingly recognized as etiologic agents of PJIs [15,16,18], they also exhibit additional clinically significant characteristics. *P. aeruginosa* and *E. coli*, in particular, is associated with higher treatment failure rates and often requires multiple surgical interventions and prolonged hospitalizations, especially when diagnosis is delayed [16,19,20].

Our SEM analyses also demonstrated that the biofilms formed by both species underwent visibly greater disruption of their extracellular matrix after application of the sonication protocol when compared with the untreated controls. This observation highlights the mechanical capacity of sonication to detach bacterial communities from the underlying surface. Similar findings were reported in a previous study, in which sonication outperformed chemical dislodgement methods for removing *E. coli* and *P. aeruginosa* biofilms from artificial surfaces [7].

In this context, diagnosing chronic PJIs poses an additional challenge, as the complexity and tolerance of bacterial biofilms increase with biofilm age [21,22]. It is also well established that, due to their matrix composition, biofilms formed by *P. aeruginosa* and *E. coli* become progressively more resilient as they mature [12]. In our study, sonication visually demonstrated its ability to disrupt both early biofilms at 24 hours (Figures S2 and S8) and mature biofilms at 72 hours (Figures S6 and S12) across all tested species. This finding may help explain the widely reported ability of sonication to enhance the sensitivity and specificity of prosthesis-associated infection diagnosis and its critical role in identifying causative pathogens in chronic or low-grade infections with negative or inconclusive PTC [8,23–26].

One of the main concerns regarding the use of sonication to disrupt biofilms from explanted implants is the potential loss of microbial viability following the procedure [14,27,28]. In this study, we observed bacterial growth on agar plates from the sonication fluid, demonstrating that the method was able to release microorganisms previously adhered to the biofilm matrix in a viable state, even after the mechanical disruption of the biofilm layer. This indicates that their capacity for growth was preserved and highlights the adhesive and structured nature of the evaluated species. Thus, our findings contribute to the literature by showing that sonication can enhance the microbiological detection of GNBs associated with implants, particularly in scenarios in which conventional methods exhibit low sensitivity [9,11,14,24,29–31].

This study has limitations inherent to the experimental model adopted. The use of an in vitro system with laboratory strains and polyethylene segments (although it enables controlled biofilm formation and direct visualization of its structure) does not fully reproduce the biomechanical and immunological complexity of the microenvironment of infected prostheses in vivo, which may influence biofilm organization and tolerance. In addition, we did not perform quantification of the bacterial load released after sonication by Colony-Forming Unit (CFU) counts, which precludes comparison of recovery efficiency between species and across different maturation stages. Nevertheless, it is important to emphasize that these limitations do not compromise the central finding of this work: the direct demonstration of sonication-mediated disruption of both young and mature biofilms, breaking their three-dimensional matrix and releasing viable cells. These results therefore provide a foundation for future investigations using clinical isolates, different prosthetic surfaces, and quantitative approaches to biofilms at varying maturation stages.

4. Materials and Methods

4.1. Bacterial Strains and Rationale for Their Selection

Laboratory reference strains of Escherichia coli (ATCC 25922) and Pseudomonas aeruginosa (ATCC 53278) were used in order to minimize phenotypic variability in biofilm-forming capacity and ensure experimental reproducibility. The use of ATCC strains also allowed controlled comparison across maturation stages, avoiding the heterogeneous biofilm behavior frequently observed in clinical isolates.

 doi:10.20944/preprints202512.1160.v1

4.2. Biofilm Formation and Experimental Design

Strains were pre-cultured in Brain Heart Infusion (BHI) broth at 37 °C for 18–24 h, after which the optical density was adjusted to approximately 1 × 10^8 CFU/mL. Three sterile segments of central venous catheter (~1.5 cm each) were added to tubes containing 2 mL of the standardized inoculum. For each strain, two experimental groups were established: (1) biofilms subjected to sonication, and (2) non-sonicated control biofilms. Additionally, negative controls consisting of sterile catheter segments incubated under identical conditions without bacterial inoculum were included to exclude contamination during handling, incubation or processing.

Biofilms were grown statically in BHI at 37 °C. The incubation times of 24 h, 48 h and 72 h were selected to represent classical stages of biofilm development: early adhesion/initial microcolonies (24 h), intermediate maturation (48 h) and mature three-dimensional architecture (72 h), as consistently described for Gram-negative biofilms. After 24 h, all samples were washed twice with sterile 0.9% NaCl to remove planktonic cells, transferred to fresh BHI medium, and incubated under the same conditions. Medium changes and washes were performed every 24 h. This procedure resulted in six experimental groups (24 h, 48 h and 72 h; each with a sonicated and non-sonicated counterpart). All experiments were performed in triplicate.

4.3. Sonication Protocol

The biofilms were processed using the standardized sonication protocol described previously [11]. Briefly, the samples were vortexed for 30 s in the collection container, ensuring complete immersion of the catheter segments in sterile 0.9% NaCl. Then, the samples were immersed in an ultrasound bath for 1 min at 40 ± 2 kHz with a power density of 0.22 ± 0.04 W/cm². Immediately after sonication, the samples were vortexed again for 30 s. Finally, approximately 15 mL of the sonication fluid (containing the catheter segments) were centrifuged at 3200 rpm for 15 min to concentrate the bacterial cells released from the biofilm for subsequent culture.

Biofilms were grown statically in BHI medium at 37 °C. After 24 hours, they were washed twice with 0.9% NaCl saline solution to remove planktonic bacteria. Then, the biofilms were transferred to fresh BHI under the same conditions and further incubated for 72 hours, with medium changes and washes every 24 hours. In this way, six groups were formed: biofilms at 24 h, 48 h and 72 h, each with a sonicated group and a control (non-sonicated) group.

A 10 µL aliquot of sonication fluid from the biofilms was plated on BHI agar and incubated at 37 °C for 18–24 hours to assess bacterial viability after mechanical disaggregation via sonication.

For scanning electron microscopy analysis, biofilm samples from all six groups were fixed in 2.5% glutaraldehyde in sodium cacodylate buffer, dehydrated through a graded ethanol series (2 minutes each step), and stored under vacuum until analysis. Prior to observation, the samples were sputter-coated with gold (MED 020, Balzer). During SEM analysis, various fields were captured in both control and sonicated samples to examine the extracellular matrix structure and to assess the effect of sonication. All procedures were performed in triplicate.

4.4. Recovery of Viable Bacteria After Sonication

A 10 µL aliquot of the processed sonication fluid was plated onto BHI agar and incubated at 37 °C for 18–24 h to assess viability of bacteria released from the biofilm matrix. Negative control samples were processed identically and all yielded negative cultures.

4.5. Scanning Electron Microscopy (SEM)

Biofilm-covered catheter segments from all experimental groups were fixed in 2.5% glutaraldehyde in sodium cacodylate buffer, dehydrated in a graded ethanol series (30%–100%; 2 min each step), and stored under vacuum until analysis. Prior to imaging, samples were sputter-coated with gold using a MED 020 (Balzer®) coating unit.

 doi:10.20944/preprints202512.1160.v1

SEM imaging was performed at the Laboratório de Microscopia Eletrônica (LME) do Instituto Avançado de Tecnologia e Inovação – ILIKA/UFPE, where several representative fields were captured from each sample to characterize the extracellular matrix and evaluate structural changes induced by sonication.

5. Conclusions

The sonication protocol proved effective in disrupting the three-dimensional architecture of Gram-negative biofilms associated with Prosthetic Joint Infections (PJI), especially Escherichia coli and Pseudomonas aeruginosa, and in releasing viable bacterial cells at all stages of biofilm maturation. These results highlight the importance of using a standardized sonication protocol as a complementary diagnostic tool for prosthesis-associated infections caused by these pathogens, particularly in chronic or low-severity cases where conventional culture methods often exhibit reduced sensitivity.

Supplementary Materials: The following supporting information can be downloaded at: https://www.mdpi.com/article/doi/s1, Figure S1. Representative SEM micrographs of 24 h control *Escherichia coli* biofilms at different magnifications (1 000 x, 2 500 x, 10 000 x, 20 000 x), Figure S2. Representative SEM micrographs of 24 h *Escherichia coli* biofilms after sonication treatment at different magnifications (1 000 x, 5 000 x, 10 000 x, 20 000 x), Figure S3. Representative SEM micrographs of 48 h control *Escherichia coli* biofilms at different magnifications (1 000 x, 5 000 x, 10 000 x, 20 000 x), Figure S4. Representative SEM micrographs of 48 h *Escherichia coli* biofilms after sonication treatment at different magnifications (1 000 x, 5 000 x, 10 000 x, 20 000 x), Figure S5. Representative SEM micrographs of 72 h control *Escherichia coli* biofilms at different magnifications (1 000 x, 8 000 x, 10 000 x, 20 000 x), Figure S6. Representative SEM micrographs of 72 h *Escherichia coli* biofilms after sonication treatment at different magnifications (1 000 x, 5 000 x, 10 000 x, 20 000 x), Figure S7. Representative SEM micrographs of 24 h control *Pseudomonas aeruginosa* biofilms at different magnifications (1 000 x, 5 000 x, 10 000 x, 20 000 x), Figure S8. Representative SEM micrographs of 24 h *Pseudomonas aeruginosa* biofilms after sonication treatment at different magnifications (1 000 x, 5 000 x, 10 000 x, 20 000 x), Figure S9. Representative SEM micrographs of 48 h control *Pseudomonas aeruginosa* biofilms at different magnifications (2 500 x, 5 000 x, 10 000 x, 20 000 x), Figure S10. Representative SEM micrographs of 48 h *Pseudomonas aeruginosa* biofilms after sonication treatment at different magnifications (950 x, 5 000 x, 10 000 x, 20 000 x), Figure S11. Representative SEM micrographs of 72 h control *Pseudomonas aeruginosa* biofilms at different magnifications (1 000 x, 5 000 x, 10 000 x, 20 000 x), Figure S12. Representative SEM micrographs of 72 h *Pseudomonas aeruginosa* biofilms after sonication treatment at different magnifications (1 100 x, 5 000 x, 10 000 x, 20 000 x).

Author Contributions: Conceptualization, N.D. and P.S.; methodology, N.D. and C.R.; validation, N.D., F.B. and P.S.; formal analysis, N.D.; investigation, N.D. and C.R.; resources, P.S.; data curation, N.D.; writing—original draft preparation, N.D.; writing—review and editing, F.A. and P.S.; visualization (SEM analysis), N.D. and F.A.; supervision, P.S.; project administration, N.D. and P.S.; funding acquisition, P.S. All authors have read and agreed to the published version of the manuscript.

Funding: The financial resources to carry out this research were provided through *Conselho Nacional de Desenvolvimento Científico e Tecnológico* – CNPq (CNPq/MCTI No. 10/2023 – UNIVERSAL).

Institutional Review Board Statement: Not applicable.

Informed Consent Statement: Not applicable.

Data Availability Statement: The SEM image dataset generated in this study is available in the Supplementary Materials. Additional full-resolution images supporting the findings of this study are available from the corresponding author upon reasonable request.

Acknowledgments: The authors acknowledge the administrative and technical support provided by the research laboratory team. During the preparation of this manuscript, the authors used ChatGPT (OpenAI, GPT-

 doi:10.20944/preprints202512.1160.v1

5.1, 2025) for text revision and language polishing. The authors have reviewed and edited all outputs and take full responsibility for the content of this publication.

Conflicts of Interest: The authors declare no conflicts of interest.

References

1. Trebše R.; Roškar S. Evaluation and interpretation of prosthetic joint infection diagnostic investigations. *Int Orthop* **2021**, *45*(4):847–855.
2. Romero I.F.; Nieto A.R. Procesamiento de muestras osteoarticulares para diagnóstico microbiológico: resultados de una encuesta multicéntrica nacional. *Enferm Infecc Microbiol Clin* **2021**, 1–5.
3. Zimmerli W.; Sendi P. Orthopaedic biofilm infections. *APMIS* **2017**, *125*(4):353–364.
4. Flemming H.-C.; Wingender J.; Szewzyk U.; Steinberg P.; Rice S.A.; Kjelleberg S. Biofilms: an emergent form of bacterial life. *Nat Rev Microbiol* **2016**, *14*(9):563–575.
5. Vrancianu C.O.; Serban B.; Gheorghe-Barbu I.; Czobor Barbu I.; Cristian R.E.; Chifiriuc M.C.; Cirstoiu C. The challenge of periprosthetic joint infection diagnosis: from current methods to emerging biomarkers. *Int J Mol Sci* **2023**, *24*(5):4320.
6. Sebastian S.; Malhotra R.; Sreenivas V.; Kapil A.; Chaudhry R.; Dhawan B. Sonication of orthopaedic implants: a valuable technique for diagnosis of prosthetic joint infections. *J Microbiol Methods* **2018**, *146*:51–54.
7. Karbysheva S. Comparison of sonication with chemical biofilm dislodgement methods using chelating and reducing agents: implications for the microbiological diagnosis of implant-associated infection. *J Am Acad Orthop Surg Glob Res Rev* **2021**, *5*(11).
8. Bellova P.; *et al*. Sonication of retrieved implants improves sensitivity in the diagnosis of periprosthetic joint infection. *BMC Musculoskelet Disord* **2019**, *20*:623.
9. Trampuz A.; Piper K.E.; Jacobson M.J.; Hanssen A.D.; Unni K.K.; Osmon D.R.; et al. Sonication of removed hip and knee prostheses for diagnosis of infection. *N Engl J Med* **2007**, *357*:654–663.
10. Oliva A.; Pavone P.; D'Abramo A.; Iannetta M.; Mastroianni C.M.; Vullo V. Role of sonication in the microbiological diagnosis of implant-associated infections: beyond the orthopedic prosthesis. *Adv Exp Med Biol* **2016**, *897*:85–102.
11. Silva N.D.S.; De Melo B.S.T.; Oliva A.; de Araújo P.S.R. Sonication protocols and their contributions to the microbiological diagnosis of implant-associated infections: a review of the current scenario. *Front Cell Infect Microbiol* **2024**, *14*:1398461.
12. Scalia A.C.; Najmi Z. Targeting bacterial biofilms on medical implants: current and emerging approaches. *Antibiotics* **2025**, *14*:802.
13. Cieslinski J.; Ribeiro V.S.T.; Kraft L.; Suss P.H.; Rosa E.; Morello L.G.; Pillonetto M.; Tuon F.F. Direct detection of microorganisms in sonicated orthopedic devices after in vitro biofilm production and different processing conditions. *J Bone Joint Infect* **2021**, *6*(2).
14. Macias-Valcayo A.; Aguilera-Correa J.-J.; Broncano A.; Parron R.; Auñon A.; García-Cañete J.; Blanco A.; Esteban J. Comparative in vitro study of biofilm formation and antimicrobial susceptibility in Gram-negative bacilli isolated from prosthetic joint infections. *Microb Drug Resist* **2023**, *29*(6):700–709.
15. Thompson J.M. Mouse model of Gram-negative prosthetic joint infection reveals therapeutic targets. *Antimicrob Agents Chemother* **2021**, *65*:e02066-20.
16. Moon Y.; Hong J.; Choi S.; Kim H.; Sohn H.M.; Jo S. Biofilm growth on different materials used in contemporary femoral head prosthesis: an in vitro study. *J Orthop Res* **2022**, *40*:1–9.
17. Benito N.; *et al*. Time trends in the etiology of prosthetic joint infections: a multicenter cohort study. *Clin Microbiol Infect* **2024**, *30*(4):547–554.
18. Fantoni M.; Borrè S.; Rostagno R.; Riccio G.; Carrega G.; Giovannenze F.; Taccari F. Epidemiological and clinical features of prosthetic joint infections caused by Gram-negative bacteria. *J Infect* **2023**, *86*(5):531–539.
19. Gonzalez M.R.; Gonzalez J.; Patel R.V.; Werenski J.O.; Lizcano J.D.; Lozano-Calderon S.A.; Gram-negative PJI Collaborative Group. Microbiology, treatment, and postoperative outcomes of Gram-negative prosthetic joint infections: a systematic review. *J Am Acad Orthop Surg* **2025**, *33*(6):e327–e339.

 doi:10.20944/preprints202512.1160.v1

20. Zouitni A.; van Oldenrijk J.; Bos P.K.; Croughs P.D.; Yusuf E.; Veltman E.S. Evaluating the clinical relevance of routine sonication for periprosthetic hip or knee joint infection diagnosis. *Antibiotics* **2024**, *13*(4):366.
21. Fernández-Sampedro M.; Fariñas-Álvarez C.; Garcés-Zarzalejo C.; et al. Accuracy of different diagnostic tests for early, delayed and late prosthetic joint infections. *BMC Infect Dis* **2017**, *17*:592.
22. Zouitni A.; Bos P.K.; Vogel M.; Croughs P.; Slobbe L.; Claus P.E.; van Oldenrijk J.; Veltman E.S.; Yusuf E. Impact of sonication fluid cultures on prosthetic joint infection diagnosis and management: a microbiology-driven evaluation using IDSA and EBJIS criteria. *Clin Infect Dis* **2025**, 391.
23. Sandbakken E.T.; Witsø E.; Sporsheim B.; Egeberg K.W.; Foss O.A.; Hoang L.; Bjerkan G.; Løseth K.; Bergh K. Highly variable effect of sonication to dislodge biofilm-embedded *Staphylococcus epidermidis* directly quantified by epifluorescence microscopy: an in vitro model study. *J Orthop Surg Res* **2020**, *15*:522.
24. Schweizer T.A.; Egli A.; Bosshard P.P.; Achermann Y. Saponin improves recovery of bacteria from orthopedic implants for enhanced ex vivo diagnosis. *Microorganisms* **2025**, *13*:836.
25. Hoekstra M.; Veltman E.S.; Nurmohamed R.F.R.H.A.; van Dijk B.; Rentenaar R.J.; Vogely H.C.; van B.C.H. Sonication leads to clinically relevant changes in treatment of periprosthetic hip or knee joint infection. *J Bone Joint Infect* **2020**, *5*:128–132.
26. Peng G.; Liu Q.; Guan Z.; *et al*. Diagnostic accuracy of sonication fluid cultures from prosthetic components in periprosthetic joint infection: an updated diagnostic meta-analysis. *J Orthop Surg Res* **2023**, *18*:175.
27. Otero J.A.; Karau M.J.; Greenwood-Quaintance K.E.; Abdel M.P.; Mandrekar J.; Patel R. Evaluation of sonicate fluid culture cutoff points for periprosthetic joint infection diagnosis. *Open Forum Infect Dis* **2024**, *11*(5):ofae159.
28. Li C.; Renz N.; Ojeda Thies C.; Trampuz A. Meta-analysis of sonicate fluid in blood culture bottles for diagnosing periprosthetic joint infection. *J Bone Joint Infect* **2018**, *3*(5):273–279.
29. Yuan Q.; Karau M.J.; Greenwood-Quaintance K.E.; Mandrekar J.N.; Osmon D.R.; Abdel M.P.; Patel R. Comparison of diagnostic accuracy of periprosthetic tissue culture in blood culture bottles to prosthesis sonicate fluid culture by Bayesian latent class modelling and IDSA PJI criteria. *J Clin Microbiol* **2018**, *56*(6):e00319-18.
30. Beguiristain I.; Henriquez L.; Sancho I.; Martin C.; Hidalgo-Ovejero A.; Ezpeleta C.; Portillo M.E. Direct prosthetic joint infection diagnosis from sonication fluid inoculated in blood culture bottles by direct MALDI-TOF mass spectrometry. *Diagnostics* **2023**, *13*(5):942.
31. Li C, Renz N, Thies CO, Trampuz A. Meta-analysis of sonicate fluid in blood culture bottles for diagnosing periprosthetic joint infection. *J Bone Jt Infect* **2018**, *3* (5):273-279. doi: 10.7150/jbji.29731.